Solid State Phenomena Vols. 141-143 (2008) pp 313-318
online at http://www.scientific.net

Predictions of Structure Breakdown, Buildup and Shear banding in Semisolid Suspensions

Andreas N. Alexandrou[1,a], Nicholas Constantinou[1] and Georgios Georgiou[2,b]

[1]Department of Mechanical and Manufacturing Engineering, University of Cyprus, Nicosia, Cyprus

[2]Department of Mathematics and Statistics, University of Cyprus, Nicosia, Cyprus

[a]andalexa@ucy.ac.cy, [b]georgios@ucy.ac.cy

Keywords: buildup; aging; coherency parameter; Herschel-Bulkley fluid; shear banding; shear rejuvenation; structural parameter; suspensions; thixotropy; yield stress

Abstract. When SSM material is subjected to a sudden transient the rate of buildup (aging) is negligible compared to the rate of breakdown (shear rejuvenation). While this is generally true, due to prolonged processing or the geometry the local shear rate in some regions may become equal or lower than the critical value, where aging becomes as important as shear rejuvenation. In this work we simulate in detail shear rejuvenation and aging in semisolid slurries. Using a standard thixotropic model used widely for modeling SSM suspensions but a novel computational method we reveal and confirm numerically for the first time shear banding. The phenomenon is found to be time dependent where the material first yields fully and then, after a certain time the yielded front retreats to form two distinct bands -one yielded and one unyielded. This phenomenon must be accounted for in the evaluation of the material constants since the time scale of the process is similar to the time scale of the phenomenon.

Introduction

In SSM suspensions there is a critical shear rate which determines the relative competition between what are known as aging and shear rejuvenation processes [1]. In shear rejuvenation the structure breaks down while during aging the microstructure slowly rebuilds after the reduction or the removal of shear. At steady state, the rates of shear rejuvenation and aging are equal. When shear is removed completely the effective viscosity reaches an infinite value and the fluid finally ceases to flow. This is the direct consequence of the fact that the viscosity, or the resistance to flow, is the result of the internal structure and the various interactions that resist large rearrangements [2-4].

The results shown below indicate the complexity of the semisolid flow even in a simple rotational rheometer. Inside the rheometer shear banding develops where the flow domain is divided into two parts: (a) the yielded region close to a shearing surface and (b) the unyielded or solid-like region. If the globally imposed shear rate increases, it is not the shear rate in the yielded region that increases, but the extent of the sheared region which increases until it includes the entire material. Hence the measured stress and the global strain rate cannot be used to extract material constants as it is customarily done. The phenomenon is also time dependent. Hence steady state material constants are not appropriate for modelling SSM processes especially at the early stages.

Theoretical model

In the literature of SSM modelling it is well established (e.g. [3]) that the rate of formation of bonds is proportional to the number of free particles in a unit volume. The rate of breakdown of inter-particle bonds is assumed to be proportional to the number of bonds. Hence, the evolution of the structure in widely described by the general form (with minor changes that do not affect the results shown here):

$$\frac{D\lambda}{Dt} = \alpha_0(1-\lambda) - \alpha_1 \lambda \dot{\gamma} e^{\alpha_2 \dot{\gamma}} \qquad (1)$$

Where λ is the coherency parameter representing the normalized number of connected bonds, α_0 is the recovery parameter, α_1 and α_2 are the breakdown parameters, $\dot{\gamma}$ is the magnitude of the rate of strain, i.e. $\dot{\gamma}$ is the second invariant of the rate of strain tensor $\mathbf{D} = \nabla\mathbf{u} + (\nabla\mathbf{u})^T$, $\mathbf{u}$ being the velocity vector. The first term in the RHS of Eq. (1) describes the aging effect and the second one accounts for the shear rejuvenation. The exponential dependence on the deformation rate is included to account for the fact that the shear stress evolution in step-up experiments is faster than in the step-down ones [6].

The suspension is described by the Herschel-Bulkley model with time-dependent properties. The material parameters of the model are assumed to be functions of λ and hence of time:

$$\boldsymbol{\tau} = \left[\frac{\tau_0(\lambda)}{\dot{\gamma}} + K(\lambda)\dot{\gamma}^{n(\lambda)-1}\right]\mathbf{D}$$

where $\boldsymbol{\tau}$ is the viscous shear stress tensor, $K(\lambda)$ is the consistency index, $n(\lambda)$ is the power-law index, and $\tau_0(\lambda)$ is the yield stress. The material parameters in the model, α_0, α_1 and α_2 and the functions $K(\lambda)$, $n(\lambda)$ and $\tau_0(\lambda)$, can be estimated as shown in [3]. For simplicity here it is assumed that these functions are constant, i.e. independent of the state of the structure. The time-dependent function $\tau_0(\lambda(t))$ must be defined a priori. In the present study, a simpler linear form is adopted

$$\tau_0(\lambda(t)) = \lambda(t)\,\tau_0$$

The flow of interest here is the classical rotational rheometer shown schematically in Fig. 1. The angular velocity of the rotating shaft is ω, thus the tangential velocity of the fluid at the shaft is $u(R_1) = \omega R_1 = U$. By using R_1, U and $K(U/R_1)^{(n-1)}$ as scales respectively for length, velocity, and stress, the dimensionless form of the conservation of linear momentum is given by

$$\mathrm{Re}\frac{\partial u}{\partial t} = \frac{1}{r^2}\frac{\partial}{\partial r}\left(r^2\tau\right), \qquad \tau = \lambda\, B + \dot{\gamma}^n, \text{ where } \dot{\gamma} = \left|r\frac{d}{dr}\left(\frac{u}{r}\right)\right|.$$

where $\mathrm{Re} = \dfrac{\rho U R_1}{K}\left(\dfrac{R_1}{U}\right)^{n-1}$ and $B = \dfrac{\tau_0}{K}\left(\dfrac{R_1}{U}\right)^{n}$ are the Reynolds and Bingham numbers, respectively.

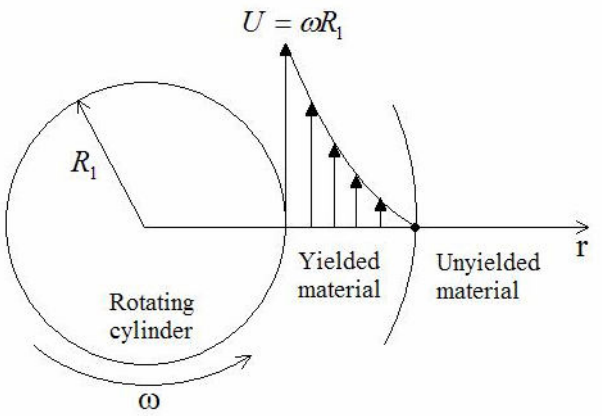

Figure 1. Schematic of the flow geometry. The material adjacent to the rotating shaft yields, while the material away from the shaft remains unyielded [2]. The outer cylinder of radius R_2 is not shown.

Results

The method of solution and the details of the discretization can be found in [2]. Since Re is a multiplying factor we only obtain results for $\mathrm{Re} = 1$. Changing its value leads only to a different time scale. Figure 2(a) shows typical experimental results for the flow in a rotational rheometer: the stress at the rotating surface after a rapid decrease follows a characteristic sigmoidal variation (in a log-log representation) and reaches steady state after a long time [5]. The time scales and values established experimentally in [5] are relevant also to those discussed here. Figure 2(b) shows the evolution of the shear rate, the shear stress, the coherency parameter and the viscosity at the rotating surface. Upon shearing the yielded domain increases rapidly to a quasi-steady-state. This growth is not associated with a significant structure breakdown. The shear stress at the rotating cylinder undergoes the same variation as obtained experimentally. On the other hand, the shear rate there from an initially large value it gradually drops to a minimum value. As soon as the yielded domain starts retreating (after its quasi-steady-state) the shear rate rises again as a result of the fluid being confined to a smaller region. Shortly after the shear rate starts decreasing, the coherency parameter reaches a minimum and the buildup term in the evolution equation increases. Therefore, the coherency parameter reaches a minimum (breakdown and buildup cancel each other out) and then increases (aging of the fluid structure) before reaching a steady-state, where the buildup and breakdown terms are equal.

Figure 3(a) shows the effect of the Bingham number on the shear stress. In general the stress level is higher for larger values of B. Figure 3(b) shows the effect of the recovery coefficient α_0. For large values of α_0 the shear stress no longer follows a sigmoidal variation but it instead drops exponentially. Figures 4(a) and 4(b) show the velocity distribution in the gap between the two concentric. The velocity varies from unity at R_1 to zero at R_2. As soon as the yielded material reaches the fixed cylinder, the velocity increases throughout the entire gap. As the shearing continues the material breaks down, the velocity decreases everywhere within the gap and shear banding occurs. When the yielded material retreats sufficiently, the velocity in the yielded region increases and reaches equilibrium when the shear band location attains a steady value. At equilibrium the velocity except close to the fixed cylinder varies almost linearly within the yielded region. Figure 5(a) shows the minimum value of B required for banding to occur as a function of the outer radius R_2. Figure 5(b) shows the effect of B, n and α_0: shear banding occurs only for parameter combinations above the corresponding curves.

Conclusions

Shear banding is a time dependent phenomenon as the material in the gap first yields fully and then after a certain time the yielded front retreats from the fixed boundary to form two distinct regions within the gap, one where the material is fully yielded and one where the material is unyielded. Interestingly the phenomenon develops in time scales similar to those found in the SSM process. Therefore shear banding in connection with structure breakdown and buildup are quite important in determining material constant for SSM slurries.

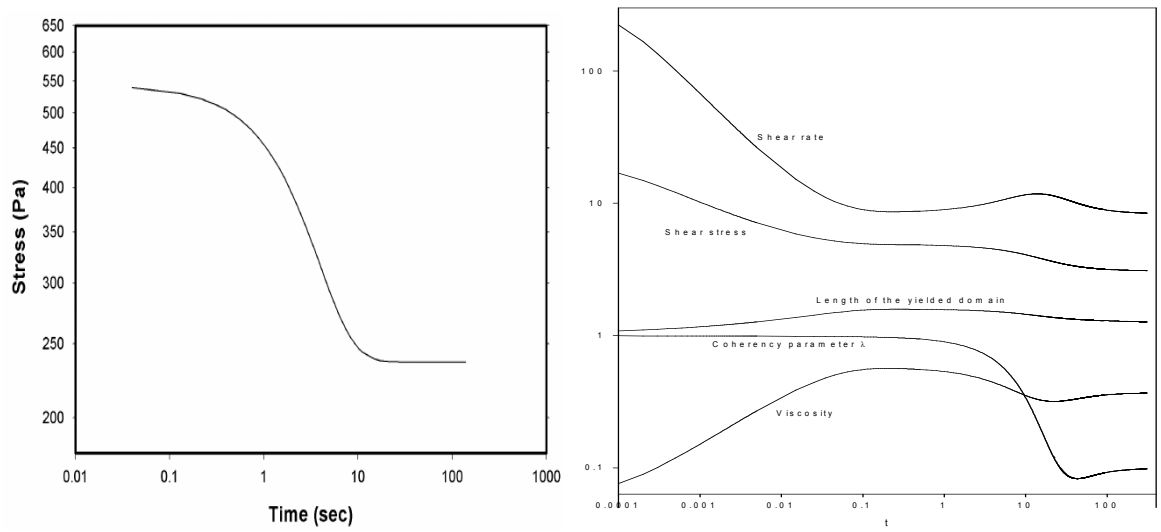

(a) (b)

Figure 2.(a) A typical result for the variation of stress with time for an SSM slurry in a rotational experiment [5]. (b) Evolution of the coherency parameter, the shear rate, the shear stress and the viscosity at the rotating surface, and of the length of the yielded domain for $B = 2$, $\alpha_0 = \alpha_1 = \alpha_2 = 0.01$ and $n = 0.5$.

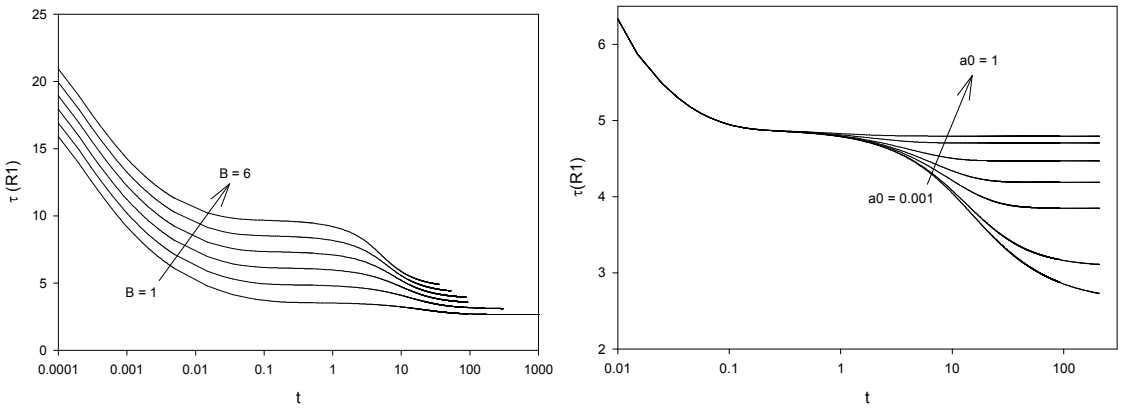

Figure 3. (a) Effect of the Bingham number B on the shear stress at the rotating surface; $\alpha_0 = \alpha_1 = \alpha_2 = 0.01$. (b) Effect of α_0 on the shear stress at the rotating surface; $B = 2$, $\alpha_0 = \alpha_1 = \alpha_2 = 0.01$, $n = 0.5$, $\alpha_0 = 0.001$, 0.01, 0.05, 0.1, 0.2, 0.5, 1.0.

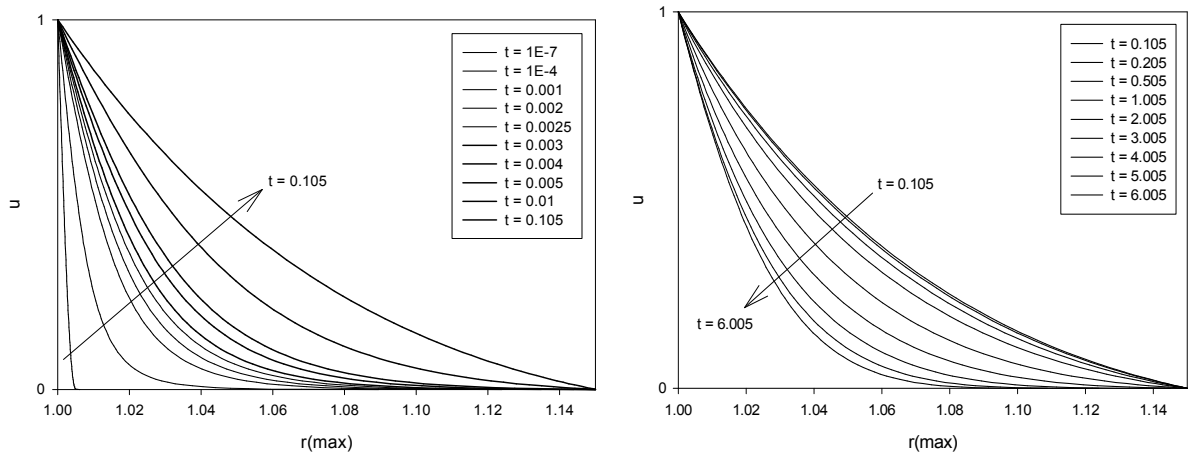

Figure 4. Evolution of the velocity distribution in the gap between the two concentric cylinders $\left(R_1 = 1,\ R_2 = 1.15\right)$. $B = 6$, $a_0 = a_1 = a_2 = 0.01$ and $n = 0.5$.

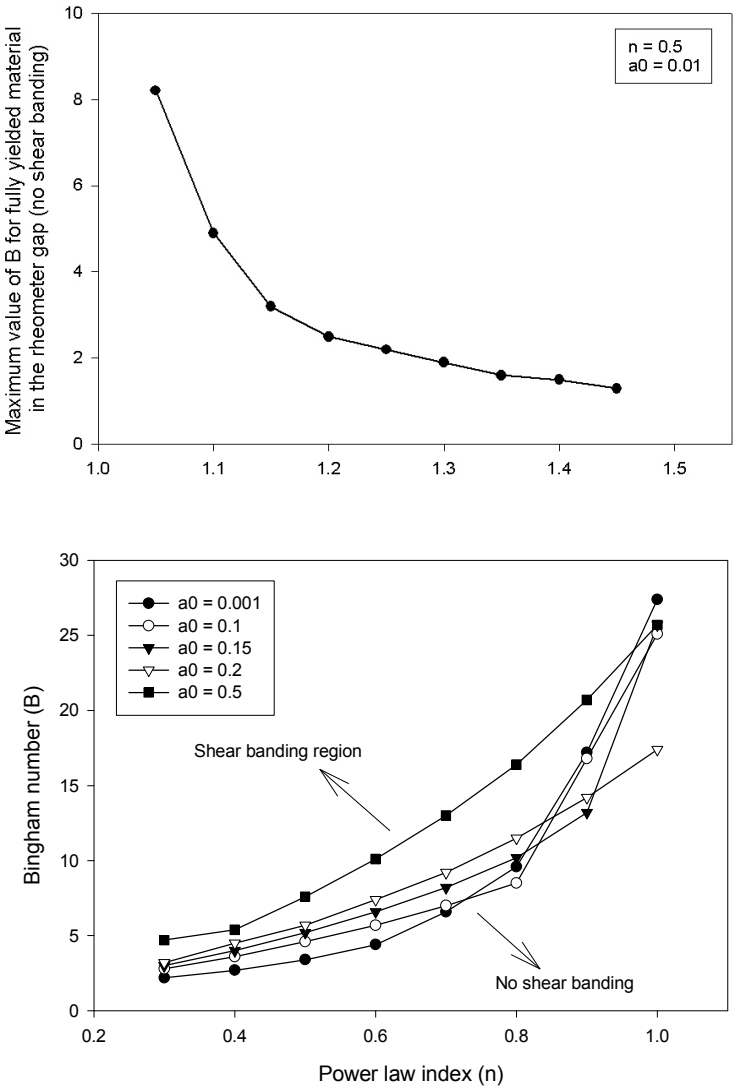

Figure 5. (a) The maximum value of B for fully yielded material (i.e. for no banding to occur) as a function of the outer radius R_2. (b) The effects of B, n and a_0: shear banding occurs only for parameter combinations above the corresponding curves.

References

[1] P. Coussot, Q.D. Nguyen, H.T. Huynh and D. Bonn, "Viscosity bifurcation in thixotropic, yielding fluids," *J. Rheol*., 46, 573–589, (2002).

[2] A.N. Alexandrou, G. Georgiou, "On the Early Breakdown of Semisolid Suspensions," *J. Non-Newtonian Fluid Mech.*, 142, 199–206, (2007).

[3] G.R. Burgos, A.N. Alexandrou, and V.M. Entov, ''Thixotropic Behavior of Semisolid Slurries," Journal of Materials Processing Technology, 110, 164-176, (2001).

[4] P.C.F. Moller, J. Mewis and D. Bonn, "Yield stress and thixotropy: on the difficulty of measuring yield stresses in practice," *Soft Matter*, 2, 274–283, (2006).

[5] N. Tonmukayakul, Q.Y. Pan, A.N. Alexandrou, D. Apelian, "Transient Flow Characteristics and Properties of Semi-solid Aluminum Alloy A356," 8th International Conference on Semi-Solid Processing of Metals and Alloys, September 21-23, 2004. Limassol, Cyprus.

[6] M. Mada, F. Ajersch, "Thixotropic Effects in Semi-Solid Al – 6%Si Alloy Reinforced with SiC particles," in Bhagat R.B. et al. (Ed.), *Metal & Ceramic Matrix Composites: Processing Modeling & Mechanical Behavior*, *The Minerals, Metals and Materials Society*, 337-350, (1990).